

# Reversibility, Pattern Formation and Edge Transport in Active Chiral and Passive Disk Mixtures

C. Reichhardt<sup>1</sup> and C. J. O. Reichhardt<sup>1, a)</sup>

*Theoretical Division and Center for Nonlinear Studies, Los Alamos National Laboratory, Los Alamos, New Mexico 87545, USA*

We numerically examine mixtures of circularly moving and passive disks as a function of density and active orbit radius. For low or intermediate densities and/or small orbit radii, the system can organize into a reversible partially phase separated labyrinth state in which there are no collisions between disks, with the degree of phase separation increasing as the orbit radius increases. As a function of orbit radius, we find a divergence in the number of cycles required to reach a collision-free steady state at a critical radius, while above this radius the system remains in a fluctuating liquid state. For high densities, the system can organize into a fully phase separated state that is mostly reversible, but collisions at the boundaries between the phases lead to a net transport of disks along the boundary edges in a direction determined by the chirality of the active disk orbits. We map the dynamic phases as a function of density and orbit radii, and discuss the results in terms of the reversible-irreversible transition found in other periodically driven non-thermal systems. We also consider mixtures of circularly driven disks and ac driven disks where the ac drive is either in or out of phase with the circular motion, and find a rich variety of pattern forming and reentrant disordered phases.

## I. INTRODUCTION

There is a wide class of nonequilibrium systems that undergo transitions from a non-fluctuating to a fluctuating state as a function of increased driving. Examples include plastic depinning, in which the transition is between a non-fluctuating pinned or well-defined flowing channel state and a strongly fluctuating plastically moving state<sup>1</sup>, periodically sheared colloidal systems<sup>2</sup>, active matter or self-driven systems<sup>3–5</sup>, the transition to turbulence in driven liquid crystals<sup>6</sup> and the general class of systems that exhibit absorbing phase transitions<sup>7</sup>. A particularly clear example of this type of behavior appears in periodically sheared dilute non-thermal colloidal particles, where at low shear or low colloid density, the system organizes into a reversible state in which the particles return to the same positions after each cycle, but when the shear or density is above a threshold value, the particles do not return and undergo long time diffusion<sup>2</sup>. Corte *et al.*<sup>8</sup> showed that although this system is always initially in an irreversible or fluctuating state, over many cycles it organizes into either a reversible state or a steady irreversible state, with the number of cycles or amount of time required to reach either of these phases diverging as a power law at a critical drive. In this case, reversible states correspond to the loss of all collisions between the particles. Further studies of periodically driven systems have revealed that reversible to irreversible transitions can also occur in more strongly interacting systems where the particles are always in contact, such as vortices in type-II superconductors<sup>9–11</sup>, dense granular matter<sup>12,13</sup>, and periodically sheared amorphous solids<sup>14–18</sup>. In dilute colloidal systems, it was shown that the particle configurations at the reversible-irreversible transition can ex-

hibit hyperuniformity<sup>19–21</sup>, and that numerous types of memory effects can arise<sup>22,23</sup>.

Active matter or self-propelled particles is another example of a nonequilibrium system that often shows transitions from strongly fluctuating disordered states to weakly fluctuating or even nonfluctuating clustered states as a function of activity or density<sup>4,5,24–26</sup>. Studies of active matter frequently employ particles that undergo run-and-tumble dynamics or driven diffusion<sup>26</sup>. Chiral active matter consisting of circularly moving particles or spinners<sup>26,27</sup> is another class of active systems that can describe biological circle swimmers<sup>26–28</sup>, self-propelled colloids<sup>27,29,30</sup>, active gears<sup>31–33</sup>, interacting rotators<sup>34,35</sup>, circularly driven particles<sup>36–40</sup>, and collections of rotating robots<sup>41</sup>.

In this work we examine a binary assembly of non-polar disks in which half the disks undergo active clockwise circular motion and the other half are passive. The system is characterized by the disk area coverage  $\phi$  and the orbit radius  $R$  of the active disks. We consider the limit of no thermal fluctuations, so the system can be trapped in a truly non-fluctuating collision-free reversible state, and we initialize the disks in a non-overlapping dilute lattice. At low disk densities, the system remains in a reversible state when the active radius is small enough, but when the active radius increases above a threshold value, a series of collisions between the active and passive disks occurs and the system organizes into a phase separated cluster or labyrinth state in which all collisions cease. The phase separation becomes stronger with increasing orbit radius, and the active disks perform circular orbits in the open regions between clusters of passive disks. At large enough orbit radius, the system remains in a permanently fluctuating state with continuous collisions. We show that the number of cycles or time required to reach a reversible state diverges at a critical orbit radius in a manner similar to that found for systems that exhibit random organization, where the time exponent is consis-

<sup>a)</sup>Corresponding author email: cjr@lanl.gov

tent with directed percolation or conserved directed percolation. At higher disk densities, the disks can organize into pattern forming or completely phase separated states in which reversible collisions occur along the boundaries between the phases. As the orbit radius increases, we find states in which the motion of the bulk regions is reversible but a net transport of disks occurs along the phase boundaries in a direction that is controlled by the chirality of the active disks. For very large orbit radii, the system again enters a fluctuating liquid state. We also examine samples in which the second species is not passive but moves under a one-dimensional (1D) ac drive, and find several distinct pattern forming states depending on whether the 1D ac drive is in or out of phase with the circular motion of the first disk species.

## II. SIMULATION AND SYSTEM

We consider a two-dimensional system with periodic boundary conditions in the  $x$  and  $y$  directions containing a total of  $N$  disks that are each of radius  $R_d$ . The system size is  $L \times L$  with  $L = 36$ , and we take  $R_d = 0.5$ . The disk-disk interactions have a repulsive harmonic form, and the force between disks  $i$  and  $j$  is given by  $\mathbf{F}_{pp}^{ij} = k(r_{ij} - 2R_d)\Theta(r_{ij} - 2R_d)\hat{\mathbf{r}}_{ij}$ , where  $r_{ij} = |\mathbf{r}_i - \mathbf{r}_j|$ ,  $\hat{\mathbf{r}}_{ij} = (\mathbf{r}_i - \mathbf{r}_j)/r_{ij}$ , and  $\Theta$  is the Heaviside step function. As in previous works<sup>42,43</sup>, we set the spring stiffness to  $k = 50$ , a value large enough to ensure that there is less than a one percent overlap between the disks. We characterize the system in terms of the total area coverage  $\phi = N\pi R_d^2/L^2$ , where a triangular solid forms when  $\phi = 0.9$ . The dynamics of the disks are determined by the following overdamped equation of motion:

$$\eta \frac{d\mathbf{r}_i}{dt} = \sum_{j \neq i}^N \mathbf{F}_{pp}^{ij} + \mathbf{F}_{circ}^i \quad (1)$$

The first term is the disk-disk interaction force and the second term is the driving force  $\mathbf{F}_{circ}$  that imposes a circular motion for  $N_A$  of the disks and is set to zero for the remaining  $N_P = N - N_A$  disks. Unless otherwise noted, we take  $N_A = N_P = N/2$ . The circular ac drive has the form  $\mathbf{F}_{circ} = \mathbf{F}_c^x + \mathbf{F}_c^y$ , where  $\mathbf{F}_c^x = A \sin(\omega t)\hat{\mathbf{x}}$  and  $\mathbf{F}_c^y = A \cos(\omega t)\hat{\mathbf{y}}$ . We fix  $\omega = 1 \times 10^{-5}$ , and vary the drive amplitude  $A$ . The damping constant  $\eta$  is set equal to unity. A single disk subjected only to the circular drive performs a clockwise circular orbit with a radius  $r_a = 2A$ . The disks are initially placed in non-overlapping positions in a diluted triangular lattice. Typically, the system starts in a transient fluctuating state and settles into a non-fluctuating or steady fluctuating state.

## III. RESULTS AND DISCUSSION

We first consider a system at a density of  $\phi = 0.424$  containing active disks labeled species 1 and passive disks

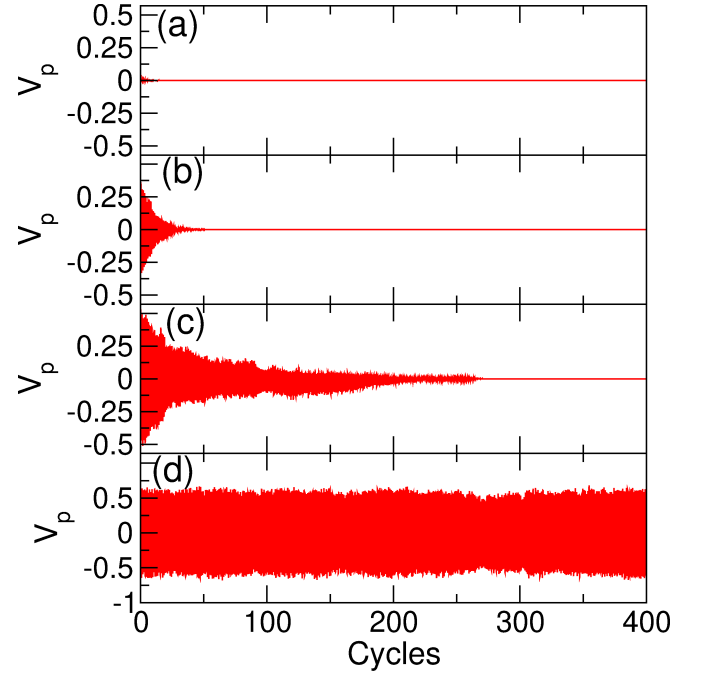


FIG. 1.  $V_p$ , the instantaneous  $x$ -component velocity of the passive disks, vs time in circular drive cycles for a binary assembly of disks in a system with a total disk density of  $\phi = 0.424$  where half of the disks are driven in a circular motion and the other half are passive. (a) At a circular drive amplitude of  $A = 0.2$ , the system is always in a collision-free state as indicated by the fixed value of  $V_p = 0.0$ . (b) At  $A = 1.5$ ,  $V_p$  is initially finite due to the occurrence of disk-disk collisions, but drops to zero after 30 cycles. (c) At  $A = 2.2$ , the system requires 250 cycles to reach a collision-free state with  $V_p = 0$ . (d) At  $A = 2.75$ , the system remains in a fluctuating state with continuous disk-disk collisions.

with  $A = 0$  labeled species 2. We measure the  $x$ -component of the instantaneous velocity of the passive species  $V_p = N_P^{-1} \sum_i^N \delta(A) (\mathbf{v}_i \cdot \hat{\mathbf{x}})$ . If the active disks collide with the passive disks,  $V_p$  will have a finite instantaneous value that fluctuates around zero; however, if there are no collisions,  $V_p = 0.0$ . If the system organizes over time into a state where there are no collisions, then  $V_p$  will initially fluctuate around zero but will converge over a number of cycles to the fixed value  $V_p = 0.0$ . In Fig. 1(a) we plot  $V_p$  versus time in circular drive cycles for the small circular drive amplitude of  $A = 0.2$ . Here we immediately obtain  $V_p = 0.0$  since the circular orbits are so small that disk-disk collisions never occur. At  $A = 1.5$  in Fig. 1(b),  $V_p$  initially has a finite value with large oscillations, produced when a large number of collisions occur between the active and passive disks, but  $V_p$  gradually decreases and reaches zero after 30 cycles, indicating that the system has organized into a collision-free state. In Fig. 1(c) at  $A = 2.2$ , it takes 250 cycles to reach a collision-free state, while at  $A = 2.75$  in Fig. 1(d), the system does not converge to a collision-free state but remains in a permanently fluctuating state.

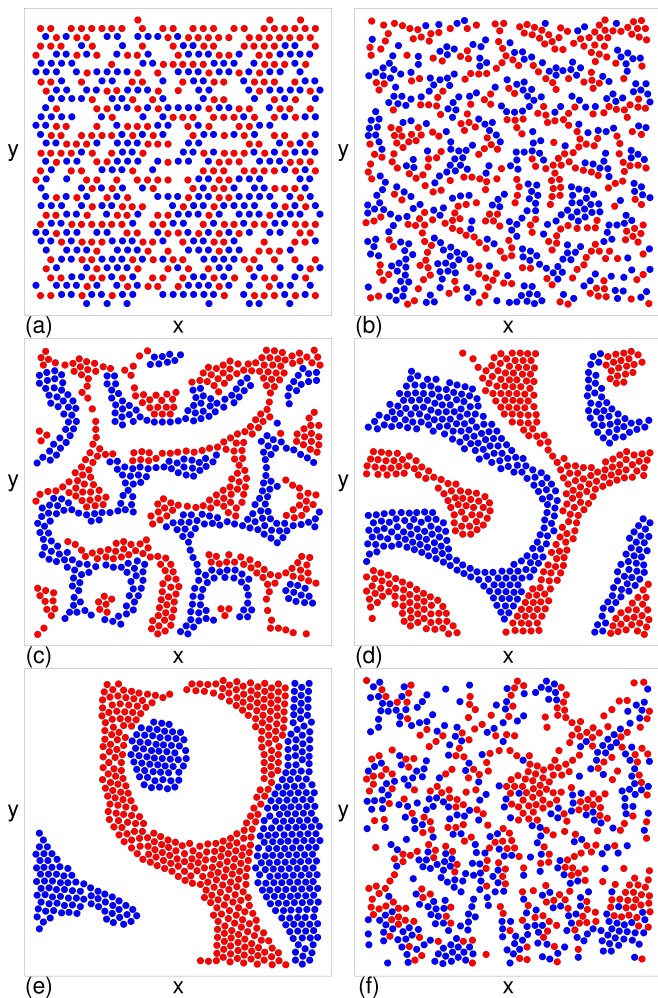


FIG. 2. Snapshot of instantaneous positions for the active (blue) and passive (red) disks for the system in Fig. 1 at  $\phi = 0.424$ . (a) At  $A = 0.1$ , the system is always in a collision-free state since the orbits of the active disks are too small for disk-disk collisions to occur, and there is no phase separation. (b) The collision-free state that forms for  $A = 0.5$  after several cycles. (c) The collision-free state at  $A = 0.75$  where we observe a partially phase separated labyrinth configuration. (d) The collision-free state at  $A = 1.5$ , where the widths of the labyrinths are larger. (e) The collision-free reversible state at  $A = 2.3$  where the phase separation is the strongest. (d) At  $A = 2.75$ , the system remains in a permanently fluctuating state with collisions between the passive and active disks.

In Fig. 2(a) we show the positions of the passive and active disks at  $A = 0.1$  where the system is always in a collision-free state since the active disk orbits are too small to produce disk-disk collisions. Here the disks remain in their initial mixed state configuration. Figure 2(b) illustrates the reversible state at  $A = 0.5$  where the disks are initially in a fluctuating state and then settle into a collision-free state in which there is some local clustering of both species. At  $A = 0.75$  in the reversible state, Fig. 2(c) shows that the system forms a phase separated labyrinth pattern containing local dense regions

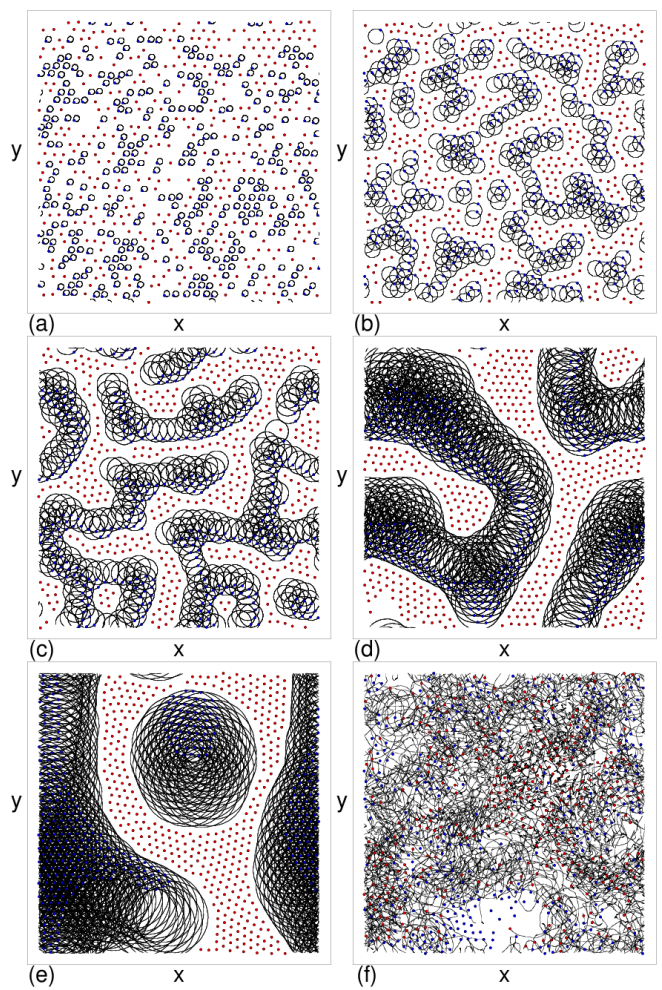


FIG. 3. Snapshot of disk positions and trajectories in the collision-free state for the active (blue) and passive (red) disks in the system in Fig. 2 at  $\phi = 0.424$ . For clarity, the disks are drawn at one-third their actual size. (a)  $A = 0.2$ . (b)  $A = 0.5$ . (c)  $A = 0.75$ . (d)  $A = 1.5$ . (e)  $A = 2.3$ . (f) The trajectories of only the passive disks in the fluctuating state at  $A = 2.5$ , where the passive disks are undergoing collisions with the active disks.

in which disks of the same species are almost touching each other. As  $A$  increases, the width of the labyrinths in the reversible state increases, as shown in Fig. 2(d) at  $A = 1.5$  for the system in Fig. 1(b) which requires 30 cycles to reach a reversible state. In Fig. 2(d) we illustrate the reversible state at  $A = 2.3$  which took 1050 cycles to form. This value of  $A$  is just below the critical value of  $A_c$ , above which the system remains in a permanently fluctuating state. We find the greatest amount of phase separation just below  $A_c$  along with considerable six-fold ordering within each phase, indicating that the local density of the dense regions is close to the solidification density of 0.9. Figure 2(f) shows a representative configuration in the fluctuating state above  $A_c$  for  $A = 2.75$ , where the clustering is lost and the disk configurations are rapidly changing.

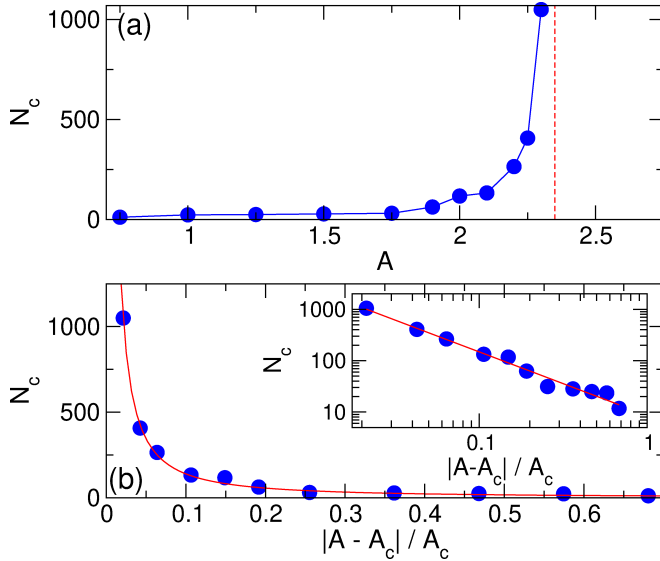


FIG. 4. (a) The number of cycles  $N_c$  required to reach a reversible state vs  $A$  for the system in Figs. 1 and 2 at  $\phi = 0.424$ .  $N_c$  diverges near  $A_c = 2.35$ , as indicated by the dashed line. (b)  $N_c$  vs  $|A - A_c|/A_c$ . The solid line is a power law fit to the form  $N_c \propto (|A - A_c|/A_c)^{-\nu}$  with  $\nu = 1.236 \pm 0.058$ . The inset shows the same plot on a log-log scale.

In Fig. 3(a-e) we highlight the trajectories of the active disks during a fixed number of cycles in the collision-free state for the system in Fig. 2 at  $\phi = 0.424$ . At  $A = 0.2$ , where Fig. 1(a) shows that the system immediately enters a collision-free state, Fig. 3(a) indicates that the circular orbits of the active disks do not overlap. In Fig. 3(b) at  $A = 0.5$ , the motion occurs in filaments with overlap in the orbits. In the reversible state the trajectories trace out the same path on every cycle. At  $A = 0.75$  in Fig. 3(c), the passive disks are confined to regions in which no active disk motion occurs. This demonstrates that the empty spaces which appear in Fig. 2(c) are periodically occupied by the active disks during each drive cycle. In Fig. 3(d), the  $A = 1.5$  system from Fig. 2(d) exhibits orbits that are much wider. Figure 3(e) again shows that in the  $A = 2.3$  system, the empty regions found in Fig. 2(e) correspond to locations through which the active disks pass during each cycle. The circular region of active disks surrounded by passive disks in the upper portion of Fig. 2(e) is actually rotating as a single group, as shown in Fig. 3(e). There are no trajectory lines associated with the passive disks in the reversible states since the passive disks are completely at rest. This is in contrast to the behavior in the irreversible state, as shown in Fig. 3(f) at  $A = 2.5$  where we highlight the trajectories of only the passive disks. The system is in a permanently fluctuating state, and the passive disks are undergoing random motion that over time produces a diffusive behavior.

In Fig. 4(a) we plot the number of cycles  $N_c$  required to reach the reversible state versus  $A$  for the

system in Figs. 1 and 2 at  $\phi = 0.424$ . There is a divergence in  $N_c$  near  $A_c = 2.35$ , as indicated by the vertical dashed line. In Fig. 4(b) we show  $N_c$  versus  $|A - A_c|/A_c$ , where the solid line is a power law fit to the form  $N_c \propto (|A - A_c|/A_c)^{-\nu}$  with  $\nu = 1.236 \pm 0.058$ . The inset shows the same data on a log-log scale. In two dimensional (2D) simulations of periodically sheared dilute colloids, the number of shearing cycles needed to reach a reversible state also exhibits a power law divergence at a critical shear amplitude with an exponent of  $\nu = 1.33$ , while in three dimensional dilute colloid experiments, the power law divergence has an exponent of  $\nu = 1.1^8$ . Other computational works for 2D periodically driven dilute disk systems give  $\nu = 1.26^{44}$ . Experiments in periodically driven vortex systems produce the value  $\nu = 1.3^{10}$ , while more recent simulations of periodically driven skyrmions and vortices show that  $\nu \approx 1.3$  on the reversible side of the transition<sup>45</sup>. In contrast, 2D simulations of amorphous solids that are in a strongly jammed state<sup>16</sup> give  $\nu = 2.53$  and  $\nu = 2.4$ , suggesting that these amorphous jammed systems fall into a different universality class. In principle, there can be another diverging time scale on the irreversible side of the transition corresponding to the time required for the system to reach a steady, rather than a transient, fluctuating state; however, the data on the irreversible side of the transition in our system is much harder to fit, so we concentrate on the behavior as the transition is approached from the reversible side. Our results are consistent with the idea that the system undergoes an absorbing phase transition, since all collisions disappear on the reversible side of the transition. Absorbing phase transitions in 2D can fall into the directed percolation universality class with  $\nu = 1.30$  or the conserved directed percolation universality class with  $\nu = 1.23^7$ . Our results are not accurate enough to distinguish between these two scenarios; however, in our system the number of disks is conserved, and the exponent we obtain is closer to that expected for conserved directed percolation.

For  $\phi < 0.5$  we find three well defined phases as a function of varied  $A$  and  $\phi$ . At low  $\phi$ , as  $A$  increases the system either remains in an initially reversible configuration, enters a reversible pattern forming state, or exhibits a permanently fluctuating state. For  $\phi > 0.5$  we observe several new sub-phases, including a pattern forming state and a completely phase separated state in which *reversible* collisions occur between some of the active and passive disks. We also find a state in which the system is reversible in the bulk but exhibits a net transport of passive disks along the boundary of the phase separated regions, meaning that the system is irreversible only along these boundary edges. In Fig. 5(a) we show the disk positions at  $\phi = 0.67$  and  $A = 0.1$  where the disks have organized to a reversible collision-free state, while in Fig. 5(b) at the same disk density and  $A = 0.75$ , a fluctuation-free reversible labyrinth state appears. At  $A = 2.0$ , illustrated in Fig. 5(c), even though the motion remains reversible, collisions occur between the ac-



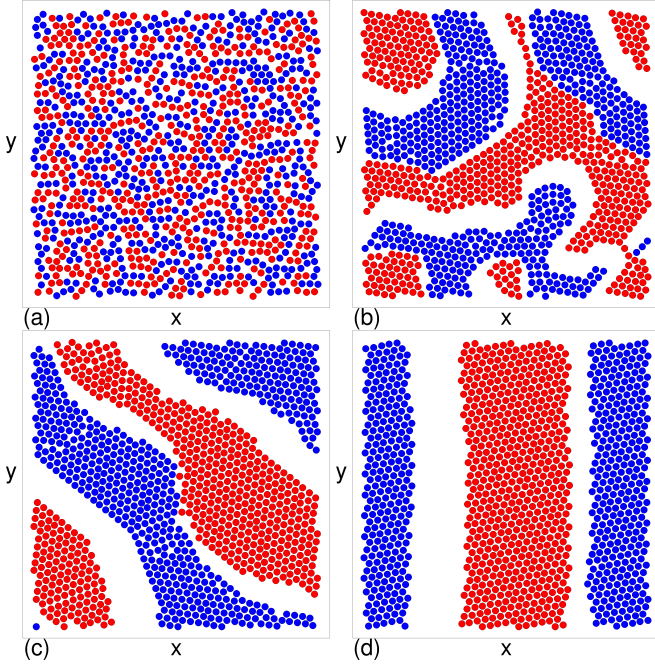


FIG. 5. Snapshot of instantaneous positions for the active (blue) and passive (red) disks at  $\phi = 0.67$ . (a) At  $A = 0.1$  the system organizes to a collision-free state. (b) At  $A = 0.75$  we find a reversible collision-free labyrinth state. (c) At  $A = 2.0$ , the system is phase separated but there are reversible collisions along the phase boundaries. (d) At  $A = 2.5$ , the system is completely phase separated and there are reversible collisions along the phase boundaries.

tive and passive disks along the boundaries of the phase separated regions. In Fig. 5(d) at  $A = 2.5$ , the system is completely phase separated, collisions between disks at the phase boundaries continue to occur, and the motion is still reversible. At this density of  $\phi = 0.67$ , for  $3.0 \leq A < 3.75$  the disks are completely phase separated but an irreversible flow of disks occurs along the phase boundaries that generates a net edge current, while for  $A > 3.75$ , the system enters a disordered state in which all the disks can diffuse.

In Fig. 6 we plot  $V_p$  versus time in circular drive cycles for the system in Fig. 5 at  $\phi = 0.67$ . At  $A = 0.1$ , shown in Fig. 6(a), there is a short transient time interval during which disk collisions and rearrangements occur before the system settles into a reversible collision-free state with  $V_p = 0.0$ , as illustrated in Fig. 5(a). In Fig. 6(b) at  $A = 2.0$ , the system is in a disordered state for the first 100 cycles, and it then settles into a completely phase separated reversible state in which  $V_p$  remains finite due to the reversible collisions occurring along the phase boundaries. We call this state the reversible collision (RC) phase. At  $A = 2.5$ , plotted in Fig. 6(c), the system initially reaches a phase separated state in which irreversible transport of disks occurs around the edges of the phase boundaries, but after 275 cycles the system settles into a RC state as shown in Fig. 5(d). When the

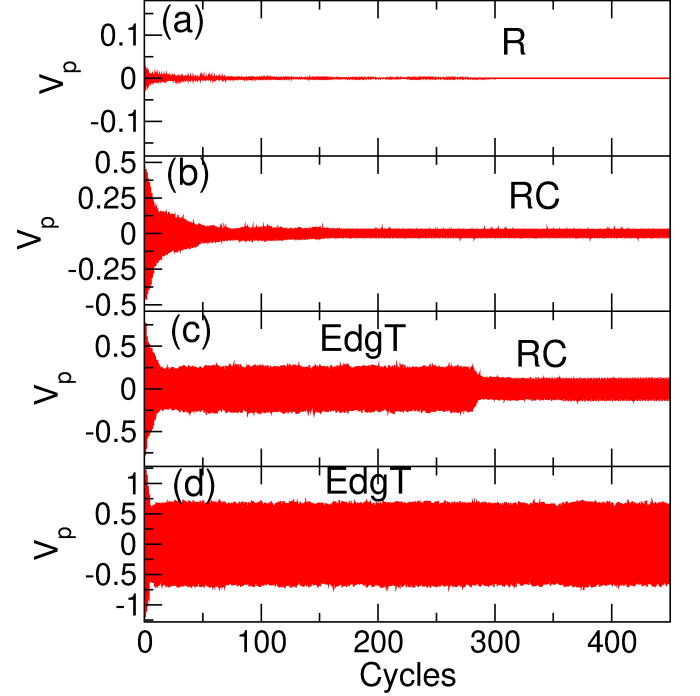


FIG. 6.  $V_p$  vs time in circular drive cycles for the system in Fig. 5 at  $\phi = 0.67$ . (a)  $A = 0.1$ , where the system forms a pattern forming reversible state with no collisions. (b)  $A = 2.0$ , where the system organizes into a completely phase separated state with reversible collisions (RC). (c)  $A = 2.5$ , where the system initially enters a completely phase separated state with edge transport (EdgT) but then transitions into a state with reversible collisions as illustrated in Fig. 5(d). (d)  $A = 4.0$ , where edge transport occurs.

edge transport is occurring,  $V_p$  exhibits large fluctuations but remains centered around zero since the edge transport runs in the positive  $y$  direction on one side of the phase boundary and in the negative  $y$  direction on the other side. In Fig. 6(d) at  $A = 4.0$ , the edge transport regime remains stable, the system never becomes fully reversible, and the fluctuations in  $V_p$  are larger. At higher drives (not shown), the system enters a liquid state and the fluctuations in  $V_p$  are even larger.

In Fig. 7(a) we show the trajectories of the active disks for a reversible motion state at  $A = 1.5$  for the  $\phi = 0.67$  system from Fig. 6. In this reversible state, disks never come into contact with each other. At  $A = 2.5$  in the same system, Fig. 7(b) shows that reversible collisions now occur between the active and passive disks along the boundaries between the two species. The large regions that are not occupied by passive disks are entirely filled by the motion of the active disks. Along the edges of the passive disk regions, passive disks undergo small periodic orbits due to collisions with the active disks, whereas in the bulk of the passive disk regions, little or no motion occurs.

In Fig. 8 we illustrate the passive disk trajectories at  $A = 2.5$  and  $\phi = 0.7272$ , where the system is completely

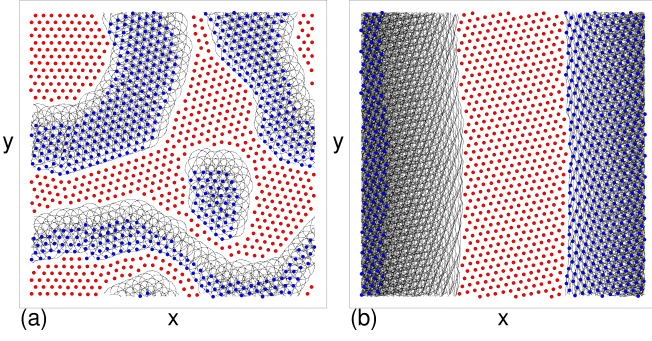


FIG. 7. Snapshot of disk positions and trajectories in the  $\phi = 0.67$  system for the active (blue) and passive (red) disks. For clarity the disks are drawn at one-half their actual size. (a)  $A = 1.5$ , where there are no collisions. (b)  $A = 2.5$ , where reversible collisions occur.

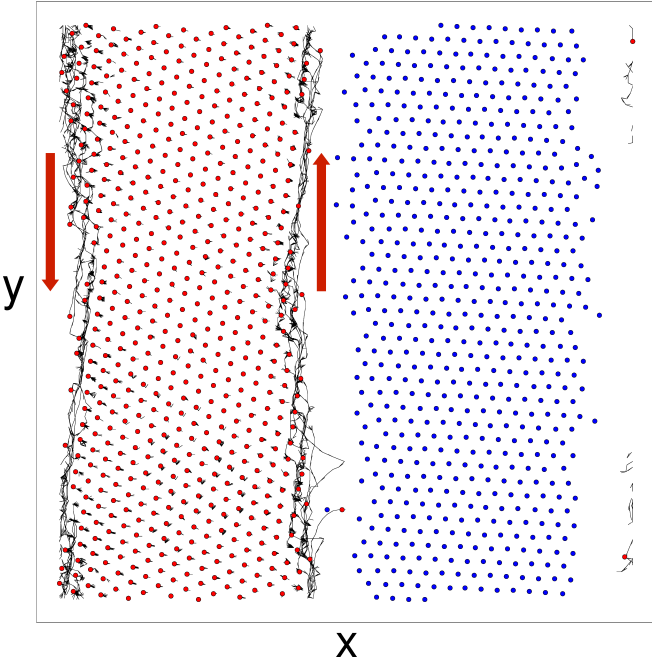


FIG. 8. Snapshot of disk positions for the active (blue) and passive (red) disks along with the trajectories of only the passive disks (lines) in a system with  $A = 2.5$  and  $\phi = 0.7272$ . The motion in the bulk of the passive disks is reversible, but a net transport of disks occurs along the edges, as indicated by the trajectories. The arrows indicate the direction of the currents. For clarity, the disks are drawn at one-third their actual size.

phase separated. In the bulk of the passive disk region, the disks move in a reversible periodic fashion, while along the edges the passive disks undergo net transport. On the right edge, the passive disks move in the positive  $y$  direction, as indicated by the arrow, while the passive disks on the left edge move in the negative  $y$  direction, giving a net current of zero. The behavior of the active disks has a similar feature, with active disks in the bulk undergoing collective periodic reversible motion, while

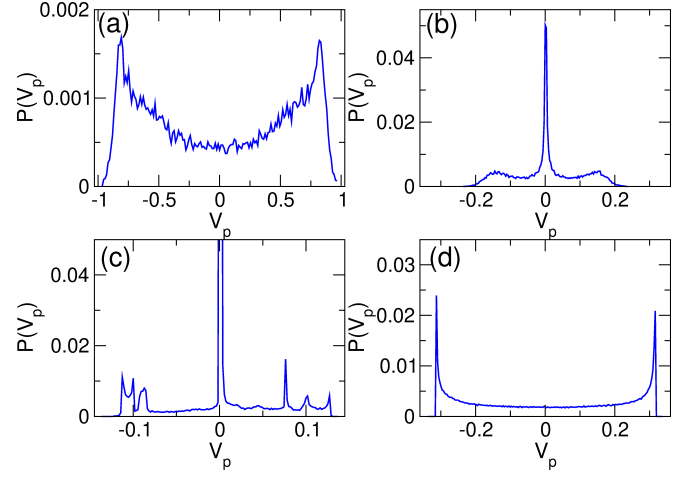


FIG. 9.  $P(V_p)$ , the distribution of the instantaneous velocities of the passive disks, after 600 circular drive cycles. (a) The fluctuating liquid state at  $A = 5.5$  and  $\phi = 0.67$ . (b)  $A = 3.5$  and  $\phi = 0.67$ , where edge transport occurs. (c)  $A = 2.5$  and  $\phi = 0.67$ , in the reversible colliding phase. (d)  $A = 0.5$  and  $\phi = 0.8847$ , where the system forms a reversible jammed state.

the active disks along the edges exhibit directed transport. The appearance of edge currents for active chiral systems has previously been observed for active spinning particles consisting of mixtures of Janus particles where one species orbits clockwise and the other orbits counterclockwise<sup>30</sup>. In the Janus particle system, partial phase separation occurs and currents appear along the phase boundaries. Edge currents have also been found in models with active spinners in confinement<sup>34</sup>, as well as in other studies of active rotators<sup>46</sup>. There are also studies of colloids undergoing oscillatory motion on patterned substrates where edge motion occurs along interfaces<sup>39</sup>.

We can characterize the different phases by analyzing the distribution of the instantaneous velocity  $P(V_p)$ . For phases in which no collisions occur,  $P(V_p)$  exhibits a single peak at  $V_p = 0.0$ . In Fig. 9(a) we plot  $P(V_p)$  after 600 circular drive cycles for a system with  $\phi = 0.67$  and  $A = 5.5$  in the fluctuating liquid state. The peaks at negative and positive values of  $V_p$  fall close to the positions expected for particles undergoing sinusoidal motion, and there is a local minimum at  $V_p = 0$ , indicating that most of the passive disks are in continuous motion. At  $A = 3.5$  in Fig. 9(b), a state with edge transport forms and there are two peaks at finite  $V_p$  that correspond to the passive disks moving along the edges as well as a large peak at  $V_p = 0.0$  produced by the stationary bulk passive disks. In Fig. 9(c) at  $A = 2.5$ , the system is in the reversible collision phase and we find a large peak at  $V_p = 0.0$  corresponding to the disks that are not colliding. Multiple smaller peaks are present at finite values of  $V_p$  due to the particular characteristics of the reversible orbits that occur during the collisions. In contrast, when there is edge transport, the motion along the boundaries is irreversible, so there are only two smeared out peaks

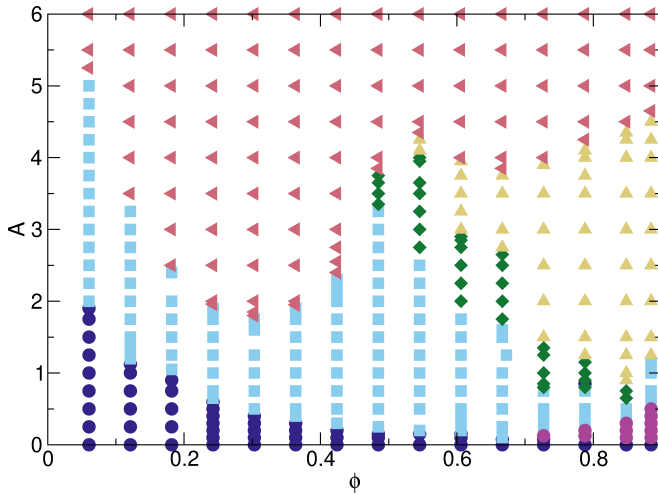


FIG. 10. Dynamic phase diagram as a function of the circular drive amplitude  $A$  vs  $\phi$  for the binary system. Dark blue circles: a mixed reversible state with no relative motion of the particles. Light blue squares: a reversible pattern forming or labyrinth state. Green diamonds: a completely phase separated state in which reversible collisions occur along the phase boundaries. Yellow triangles: a phase separated state that exhibits edge transport. Dark pink triangles: a fluctuating liquid state. Magenta circles: a reversible jammed state.

as shown in Fig. 9(b). In a sample with  $\phi = 0.8847$  and  $A = 0.5$ , the system forms a reversible jammed state in which all the particles move together rigidly, and Fig. 9(d) indicates that the shape of  $P(V_p)$  matches what would be expected for completely sinusoidal motion.

By conducting a series of simulations for varied  $\phi$  and  $A$  and examining the behavior of  $V_p$  and the images, we construct a dynamic phase diagram as a function of  $A$  vs  $\phi$ , as shown in Fig. 10. At small  $\phi$  and small  $A$ , the system immediately enters a non-interacting mixed state. This state extends over the largest range of  $A$  when  $\phi$  is small, since under these conditions the distance between adjacent disks is large and thus it is necessary for  $A$  to be relatively large in order for the disks to contact each other. In the region marked with light blue squares, a reversible pattern forming or labyrinth state appears which reaches its widest extent at  $\phi = 0.484$ . The diamonds indicate the completely phase separated RC state in which the passive and active particles undergo collisions but the system remains reversible. The yellow triangles show the regime containing phase separated states that undergo edge transport, the dark pink triangles mark the disordered states, and the magenta circles appearing at large  $\phi$  show the presence of what we call a reversible jammed state.

An example of a pattern forming reversible phase that appears for  $\phi > 0.67$  is illustrated in Fig. 11(a) at  $\phi = 0.848$  and  $A = 0.5$ . In this state, collisions between the disks occur yet the motion remains reversible. We do not distinguish such states from the pattern forming states that form without collisions between disks.

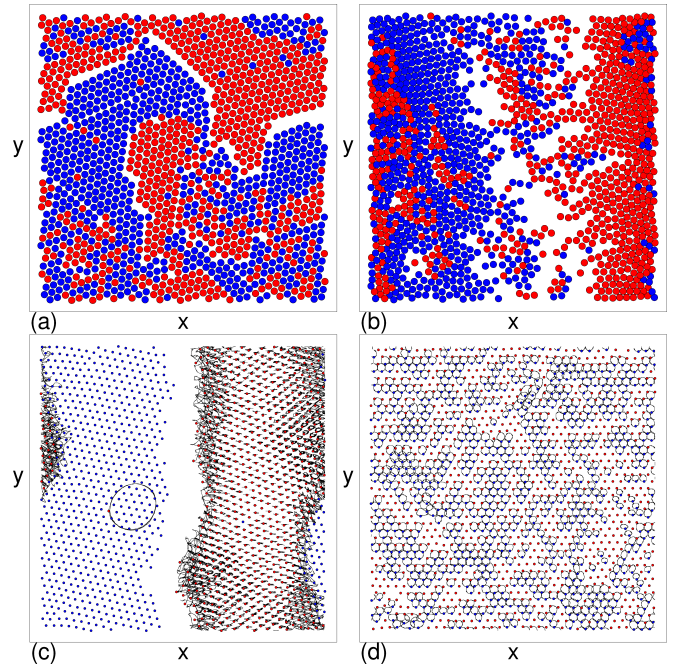


FIG. 11. (a, b) Snapshot of instantaneous positions for the active (blue) and passive (red) disks. (a) At  $\phi = 0.848$  and  $A = 0.5$ , there is a pattern forming state in which the particles exhibit reversible collisions. (b) At  $\phi = 0.848$  and  $A = 5.0$ , we find a fluctuating state where some local phase separation occurs. (c) Snapshot of disk positions and passive disk trajectories during five circular drive cycles for the active (blue) and passive (red) disks in the edge transport state at  $\phi = 0.848$  and  $A = 1.5$ . For clarity, the disks are drawn at one-third their actual size. There is a single passive disk that has become trapped in the active disk cluster, and it rotates with the active cluster as indicated by the large circular orbit. (d) Snapshot of disk positions and active disk trajectories for the active (blue) and passive (red) disks in the reversible jammed state for the system in Fig. 9(d) at  $\phi = 0.8847$  and  $A = 0.5$  where there is no mixing relative to the initial configurations but the disks undergo reversible motion and the entire system moves as a rigid solid.

For  $\phi < 0.484$ , the disordered or liquid state that appears at higher  $A$  is generically strongly mixed, while for  $\phi > 0.484$ , the disordered phase exhibits a partial phase separation of the type illustrated in Fig. 11(b) at  $\phi = 0.848$  and  $A = 5.5$ , even as all of the disks undergo diffusive behavior at long times. For  $\phi > 0.67$ , there is a window in which the disks remain in their initially diluted triangular configuration but undergo no mixing, producing a state that can be viewed as reversibly jammed, as illustrated in Fig. 9(d) and Fig. 11(d). At higher  $\phi$ , near but below the  $\phi = 0.9$  crystallization density, a small but finite  $A$  causes the effective radius of the active disks to be larger than the actual radius, so the system behaves as though it has reached the crystallization density, leading to the formation of the reversible jammed state. Once  $A$  becomes large enough, however, plastic rearrangements occur and produce a partial phase separation.



The studies described here were performed in the absence of thermal fluctuations. It is possible that including thermal fluctuations would permit some portion of the pattern forming phases to become completely phase separated over time. Thermal fluctuations would cause the disordered liquid phases to expand, and similarly the regions containing edge currents could also expand. We note that in studies of chiral polar mixtures, regions of ordered and disordered phases were observed as functions of various parameters<sup>40</sup>; however, several of the phases we find for non-polar mixtures do not appear for the polar chiral particles<sup>40</sup>. Active systems containing run and tumble or driven diffusive active particles in which there is a mixture of active and passive particles or multiple active species with different mobilities also exhibit phase separated and partially phase separated states of the different species<sup>47–50</sup>.

The evidence for the existence of an absorbing phase transition is strongest for  $\phi < 0.5$  from the reversible collision-free state to the fluctuating liquid state. We have not been able to identify clear time scales for the transition from the reversible pattern forming states to the phase separated states. This transition is more subtle since the time scales in this case could be related to coarsening dynamics rather than to a potential absorbing phase transition. We are also not able to determine whether the transitions from the phase separated states with or without edge transport into the fluctuating liquid phase also show a diverging time scale. Such a measurement is complicated to perform in states with edge transport, since we often observe that the width of the region in which the irreversible edge current flows grows for higher  $A$ , as illustrated in Fig. 11(c) for a sample with  $\phi = 0.848$  and  $A = 1.5$ , before completely disappearing at higher  $A$ .

In Fig. 11(a) we show the disk configurations in the reversible pattern forming phase at  $\phi = 0.848$  and  $A = 0.5$  where large regions of triangular ordering appear. There are several active disks that have become trapped in the bulk region of passive disks and are unable to move or escape. Similarly, we find an occasional passive disk that is trapped in the bulk region of active disks and rotates in synchrony with the active disks. Figure 11(b) illustrates the disordered or liquid phase at  $\phi = 0.848$  and  $A = 5.0$ , where the system tends to phase separate but mixing of the disk species still occurs, and the passive disks undergo diffusive motion at long times. In Fig. 11(c), an edge transport state at  $\phi = 0.848$  and  $A = 1.5$  contains a passive disk trapped in the bulk of the active disks that moves in a circular orbit, while the remaining passive disks exhibit significant motion only along the phase boundary between passive and active disks along with a small circular motion in the bulk. Figure 11(d) shows the trajectories for the active particles at  $\phi = 0.8847$  and  $A = 0.5$  from the system in Fig. 9(d) in a reversible jammed state where there is no phase separation beyond the initial configuration but the disks are reversibly colliding and the entire system rotates as a rigid solid.

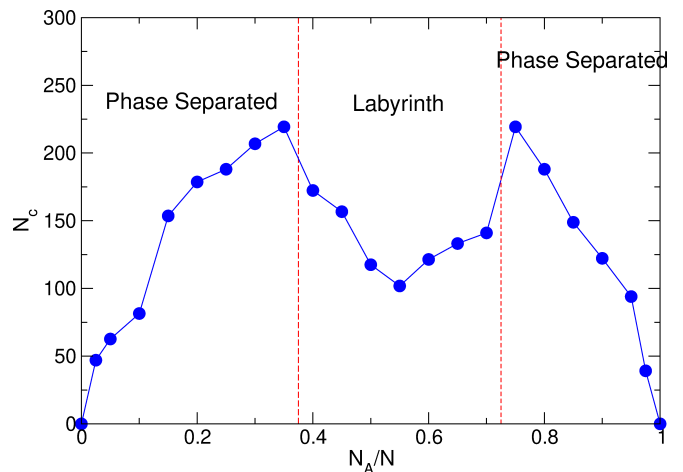


FIG. 12.  $N_c$ , the number of drive cycles required to reach a collision-free state, versus the fraction of active particles  $N_A/N$  for a system with  $\phi = 0.424$  and  $A = 2.0$ . For  $N_A/N \leq 0.35$ , the system forms a stripe structure as illustrated in Fig. 13(c), while for  $0.35 < N_A/N < 0.75$ , a labyrinth state appears as shown in Fig. 13(a,b). For  $N_A/N > 0.75$  the system enters another phase separated stripe state of the type shown in Fig. 13(d).

We have also considered varied ratios of active to passive disks and in general find similar results. In Fig. 12 we plot  $N_c$ , the number of cycles required to reach a reversible state in which all collisions are lost, versus the fraction of active particles  $N_A/N$  for a system in which we fix the total disk density and drive to  $\phi = 0.424$  and  $A = 2.0$ , respectively. We find that  $N_c$  is small when  $N_A/N < 0.1$  or  $N_A/N > 0.9$  since most of the disks are already effectively phase separated into regions containing only the majority species. A local minimum in  $N_c$  appears near  $N_A/N = 0.5$  in the labyrinth state, while there are local maxima in  $N_c$  near  $N_A/N = 0.35$  and  $N_A/N = 0.75$  at the transitions between the phase separated and labyrinth states. At the  $N_c$  minimum falling at half filling, the amount of demixing that needs to occur is largest since there are equal numbers of each disk species, but the magnitude of the fluctuations in the system is also largest due to collisions between different disk species, and as a result the system can rapidly explore phase space in order to reach a reversible state. We find a weak asymmetry around  $N_A/N = 0.5$  in which  $N_c$  is slightly higher for  $0.5 - \delta N_A/N$  compared to its value for  $0.5 + \delta N_A/N$ , where  $\delta N_A/N < 0.1$ . This is a result of the reduced amount of fluctuations in the system when the number of active disks is smaller than 50% compared to when it is higher than 50%, and the system can more rapidly reach a reversible state when the fluctuations are larger. Labyrinth patterns appear when  $0.35 < N_A/N < 0.75$ , as indicated by the dashed lines in Fig. 12, while outside of this window strongly phase separated configurations form. In Fig. 13(a) we illustrate the collision-free state for the system in Fig. 12 at  $N_A/N = 0.4$ , and in Fig. 13(b) we show the sys-



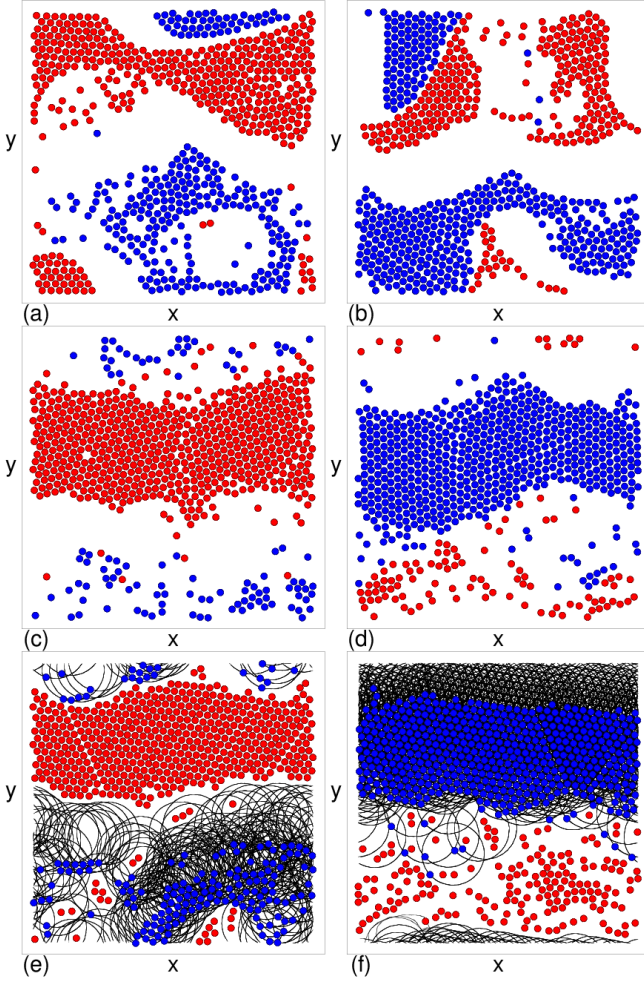


FIG. 13. (a-d) Snapshot of instantaneous positions for the active (blue) and passive (red) disks for the system in Fig. 12 at  $\phi = 0.424$  and  $A = 2.0$ . (a)  $N_A/N = 0.4$ . (b)  $N_A/N = 0.6$ . (c)  $N_A/N = 0.15$ . (d)  $N_A/N = 0.85$ . (e, f) Snapshot of disk positions and active disk trajectories for the active (blue) and passive (red) disks in the same system at (e)  $N_A/N = 0.25$  and (f)  $N_A/N = 0.75$ .

tem at  $N_A/N = 0.6$ . In each case we find a labyrinth pattern, and the smallest labyrinth widths appear for  $N_A/N = 0.5$ . The collision-free state at  $N_A/N = 0.15$  is shown in Fig. 13(c), where the passive disks form a single dense cluster or stripe with mostly triangular ordering while the active disks form a non-clustered disordered arrangement. At  $N_A/N = 0.85$  in Fig. 13(d), the active disks form a dense cluster and the passive disks are in disordered positions. The peaks in  $N_c$  in Fig. 12 correspond to disk ratios for which the system first starts to form single domains instead of labyrinths, indicating that there is a competition between the two different types of pattern formation.

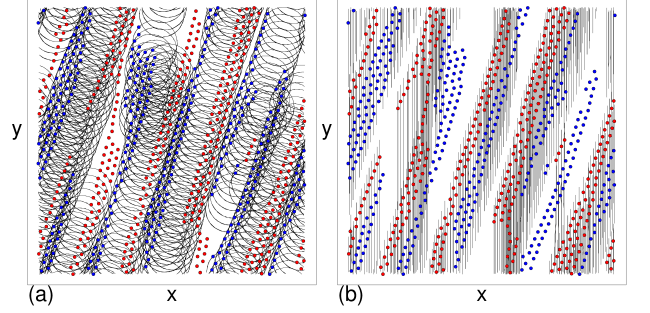


FIG. 14. Snapshot of disk positions and trajectories for species one (blue) and species two (red) disks in a system with  $\phi = 0.4242$  where species one undergoes clockwise circular motion with  $A = 1.5$  and species two undergoes  $y$ -direction ac driving with  $A_2 = 4.0$ . For clarity, the disks are drawn at one-half their actual size. The drives of the two species are in phase. (a) Trajectories of only species one showing circular orbits. (b) Trajectories of only species two showing 1D motion.

#### IV. OTHER TYPES OF DRIVING

We next consider the case where  $N_A = N/2$  and both disk species are driven. When all the disks are active with the same chirality, driving amplitude, and driving frequency, there are no disk-disk collisions and the system rotates in unison as a whole. If the second disk species moves counterclockwise while the first disk species moves clockwise, we observe the same behavior found for mixtures of active and passive disks, except that the values of  $A$  and  $\phi$  at which the reversible to irreversible transition appears shift downward. If the second species is subjected to a one-dimensional  $y$ -direction ac drive instead of a circular drive, while the first species continues to undergo circular motion, we observe several different phases depending on whether the ac drive is in or out of phase with the circular drive.

We first consider the case in which disk species two experiences a  $y$ -direction ac drive that is in phase with

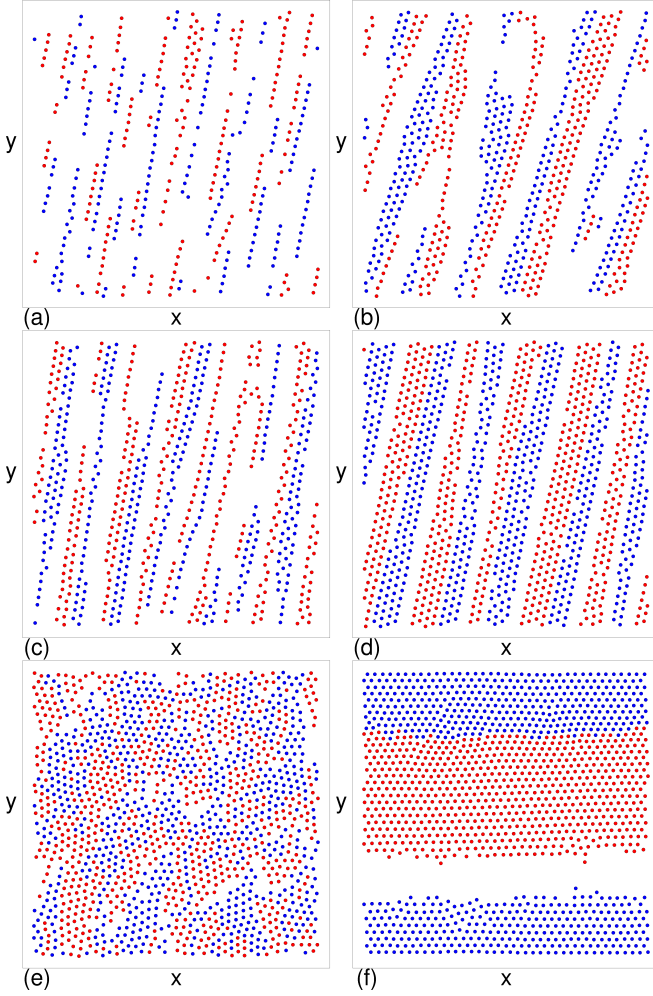


FIG. 15. Snapshot of instantaneous positions for the circularly driven species one disks (blue) and ac driven species two disks (red) for a system with  $A = 1.5$  in which the two species move in phase. For clarity, the disks are drawn at one-half their actual size. (a) Reversible laned state at  $A_2 = 7.0$  and  $\phi = 0.182$ . (b) Reversible laned state at  $A_2 = 4.0$  and  $\phi = 0.4242$ , which is also illustrated in Fig. 14. (c) Reversible laned state at  $A_2 = 7.0$  and  $\phi = 0.4242$ . (d) Laned state at  $A_2 = 7.0$  and  $\phi = 0.67$ . (e) Fluctuating liquid phase at  $A_2 = 7.0$  and  $\phi = 0.848$ . (f) A completely phase separated state at  $A_2 = 1.5$  and  $\phi = 0.848$ .

the circular ac drive of species one, such that  $F_2^y = A_2 \cos(\omega t) \hat{y}$ . Here  $\omega$  has the same value for both disk species. In Fig. 14(a) we plot the positions of all the disks and the trajectories of only the species one circularly driven disks for a sample with  $\phi = 0.4242$ ,  $A = 1.5$ , and  $A_2 = 4.0$ . Figure 14(b) shows the same state with only the trajectories of the species two ac driven disks. At this value of  $A$  we observe a new vertical stripe or laned phase that is absent when the species two disks are passive. As we vary  $\phi$ , we also observe a fluctuating disordered state and phase separated states. In Fig. 15(a) we plot the disk positions in a sample with  $\phi = 0.182$ ,  $A = 1.5$ , and  $A_2 = 7.0$ , which is initially in a disor-

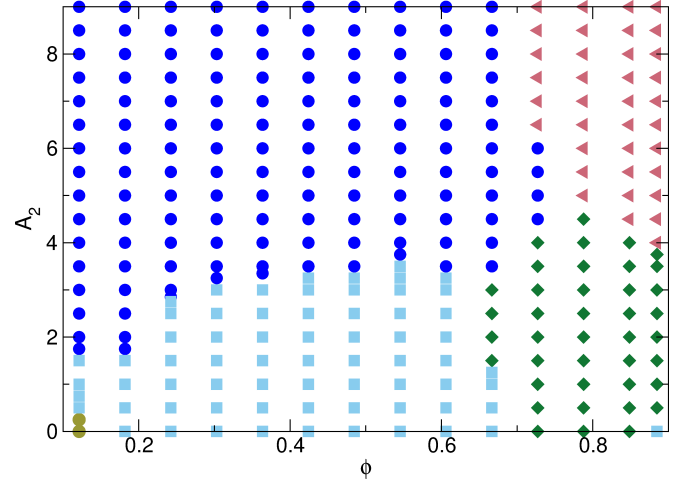


FIG. 16. Dynamic phase diagram as a function of  $A_2$  vs  $\phi$  for a system in which species one disks undergo clockwise circular motion with  $A = 1.5$  and species two disks are subjected to a  $y$ -direction ac drive of amplitude  $A_2$ . Dark blue circles: reversible laned state. Light blue squares: reversible pattern forming state. Green diamonds: completely phase separated state. Dark pink triangles: fluctuating liquid state. Light green circles: initial reversible state. Here we do not distinguish the fully phase separated states that exhibit edge transport from those that do not exhibit edge transport.

dered state but organizes over time into a collision-free reversible laned state in which the particles are aligned along the  $y$ -direction. In Fig. 15(b) at  $\phi = 0.424$  and  $A_2 = 4.0$ , which is also illustrated in Fig. 14, the lanes are thicker and there is a tendency for the two species to cluster together. At  $A_2 = 7.0$  in Fig. 15(c), the width of the lanes is reduced, while in Fig. 15(d) at  $\phi = 0.67$  and  $A_2 = 7.0$ , the lanes are wider. In general we find that as  $A_2$  increases, the lanes become thinner, while the lanes get thicker as  $\phi$  increases. The laned states for  $\phi < 0.5$  are collision-free, while for  $\phi > 0.5$ , reversible disk-disk collisions can occur. In Fig. 15(e) at  $\phi = 0.848$  and  $A_2 = 7.0$  we find a fluctuating liquid state without lanes, while in Fig. 15(f) at  $\phi = 0.848$  at  $A_2 = 1.5$ , a fully phase separated state appears. In general, when the drives of the two species are in phase, the edge transport that occurs in the fully phase separated states is weaker compared to the edge transport exhibited by passive species two disks.

In Fig. 16 we plot a dynamic phase diagram as a function of  $A_2$  versus  $\phi$  for the system in Figs. 13 and 14 in which species one undergoes circular motion with  $A = 1.5$ . We find a laned state, a pattern forming state, a phase separated state, a fluctuating phase, and the initial reversible state in which the particles do not rearrange. Here we do not distinguish phase separated states that have edge transport from those that do not have edge transport. We have also varied  $A$  in addition to varying  $A_2$  and observe phases similar to those illustrated in Fig. 16, but find in general that the fully phase separated

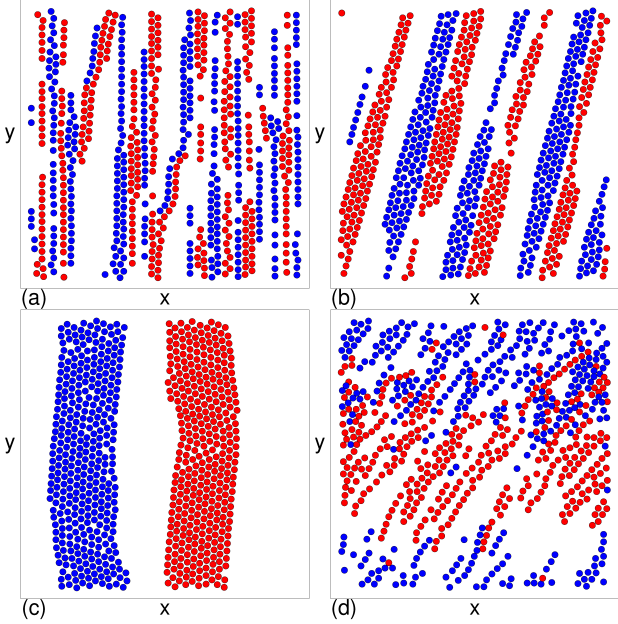


FIG. 17. Snapshot of instantaneous positions for the circularly driven species one disks (blue) and ac driven species two disks (red) for systems with  $\phi = 0.4242$  and  $A_2 = 7.0$ . (a)  $A = 0.0$ . (b)  $A = 2.5$ . (c)  $A = 4.5$ . (d)  $A = 8.0$ .

state remains stable for much lower values of  $\phi$  compared to systems in which the species two disks are passive. In Fig. 17(a) we plot the disk positions for a system with  $\phi = 0.4242$  at  $A = 0.0$  and  $A_2 = 7.0$ . A laned state appears in which the lanes are aligned in the  $y$  direction, parallel to the ac drive on the species two disks. This is distinct from the laned state that forms at finite  $A$  in which the lanes are tilted, as illustrated in Fig. 17(b) for  $A = 2.5$  and  $A_2 = 7.0$ . In Fig. 17(c) at  $A = 4.5$  and  $A_2 = 7.0$ , complete phase separation occurs, while in Fig. 17(d) at  $A = 8.0$  and  $A_2 = 7.0$  we find a fluctuating liquid state.

We next consider samples in which the ac drive on species two is out of phase with the circular drive of species one, so that  $F_2^y = A_2 \sin(\omega t) \hat{y}$ . Placing the two drives out of phase tends to increase the frequency of collisions between the particles. It also produces the interesting effect of several reentrant phases, such as reversible behavior for low and high values of  $A_2$  but irreversible behavior at intermediate values of  $A_2$ . An example of this appears in Fig. 18(a) where we plot  $V_2$ , the instantaneous  $x$  component velocity of the species two disks, versus time in number of ac drive cycles for a system with  $\phi = 0.242$ ,  $A = 1.5$ , and  $A_2 = 0.5$ . Initially the

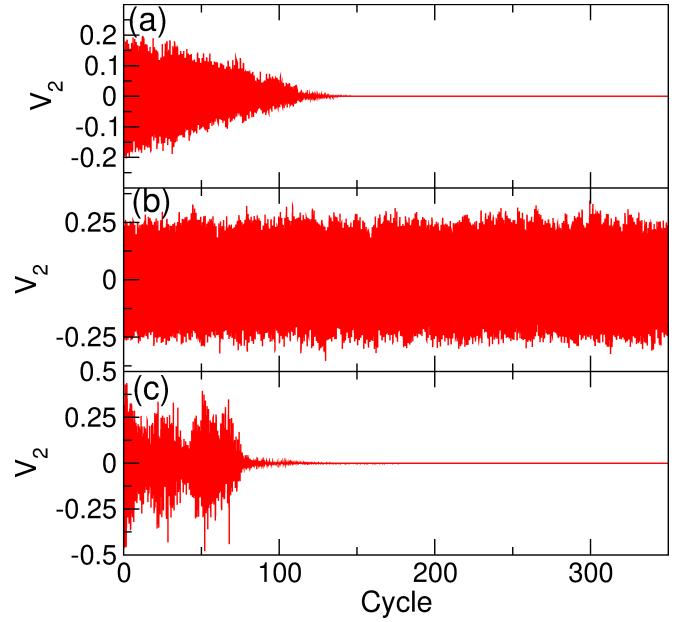


FIG. 18.  $V_2$ , the instantaneous  $x$ -component velocity of the species two disks, vs time in ac drive cycles for a system in which the species one disks are circularly driven and the species two disks experience a  $y$ -direction ac drive that is out of phase with the species one drive. Here  $\phi = 0.242$  and  $A = 1.5$ . (a) At  $A_2 = 0.5$ , the system organizes into a collision-free pattern forming state. (b) At  $A_2 = 4.0$ , the system remains in a fluctuating state. (c) At  $A_2 = 8.0$ , the system forms another reversible collision-free state.

disks are in a fluctuating state, but after 110 cycles, they settle into a collision-free reversible state with  $V_2 = 0.0$ . We note that the instantaneous  $y$  component velocity of the species two disks (not shown) has strong periodic oscillations due to the ac drive. For this value of  $A_2$ , the reversible state is a pattern forming state similar to those previously shown. In the same system at  $A_2 = 4.0$ , Fig. 18(b) shows that the sample remains in a fluctuating state as illustrated in Fig. 19(a), while at  $A_2 = 8.0$  in Fig. 18(c), the system settles into a collision-free reversible state. The reversible state at  $A_2 = 8.0$  appears in Fig. 19(b). It differs from the pattern forming state found at lower  $A_2$  since it is composed of a series of single-species vertical stripe segments of alternating species type, and the stripe segments themselves form a higher order diagonal stripe. We label this phase a mixed laned state. In Fig. 19(c) we show the disk configurations at  $\phi = 0.4242$  and  $A_2 = 3.5$  where the system forms a phase separated state, while in Fig. 19(d) at the same density and  $A_2 = 8.0$ , a fluctuating liquid phase appears. Figure 19(e) shows a phase separated state with edge transport at  $\phi = 0.848$  and  $A_2 = 4.5$ , while in Fig. 19(e), a sample with the same density and  $A_2 = 8.0$  is in a liquid state that has undergone partial phase separation.

In Fig. 20 we construct a dynamic phase diagram as a function of  $A_2$  versus  $\phi$  for the system in Figs. 18 and 19 at fixed  $A = 1.5$ . We find a reversible initial state, a



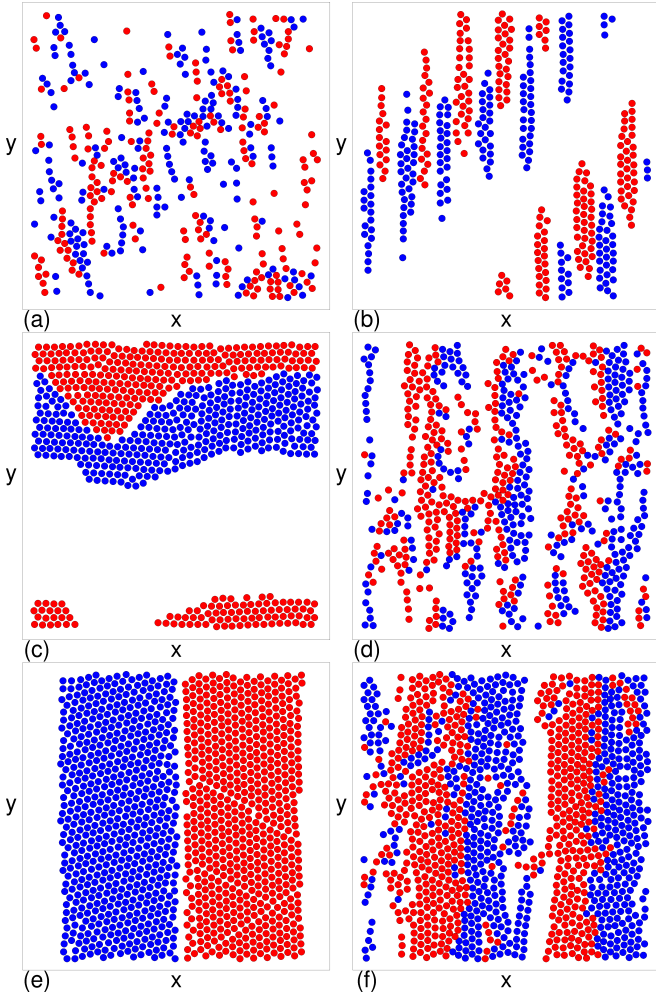


FIG. 19. Snapshot of instantaneous positions for the circularly driven species one disks (blue) and ac driven species two disks (red) in the system from Fig. 18 where the two species are moving out of phase. (a) Irreversible state at  $\phi = 0.242$  and  $A_2 = 4.0$ . (b) Reversible mixed laned state at  $\phi = 0.242$  and  $A_2 = 8.0$ . (c) Phase separated state at  $\phi = 0.424$  and  $A_2 = 3.5$ . (d) Fluctuating state at  $\phi = 0.424$  and  $A_2 = 8.0$ . (e) Phase separated state with edge transport at  $\phi = 0.848$  and  $A_2 = 4.5$ . (f) Partially phase separated fluctuating liquid at  $\phi = 0.848$  and  $A_2 = 8.0$ .

pattern forming state, fully phase separated states that can be completely reversible or have edge transport, a fluctuating state, and a reversible mixed laning state. A reentrant phenomena appears for  $\phi < 0.5$  when the low  $A_2$  reversible pattern forming state is followed by an intermediate irreversible state that transitions into a reversible state of either the mixed lane or phase separated type. At  $\phi = 0.303$ , the system transitions from a reversible pattern forming state to a fluctuating state, than into a phase separated state, and finally back to an irreversible fluctuating state as a function of increasing  $A_2$ . We generally find larger regions of fluctuating states when the drives of the two species are out of phase compared to when they are in phase. We have also ex-

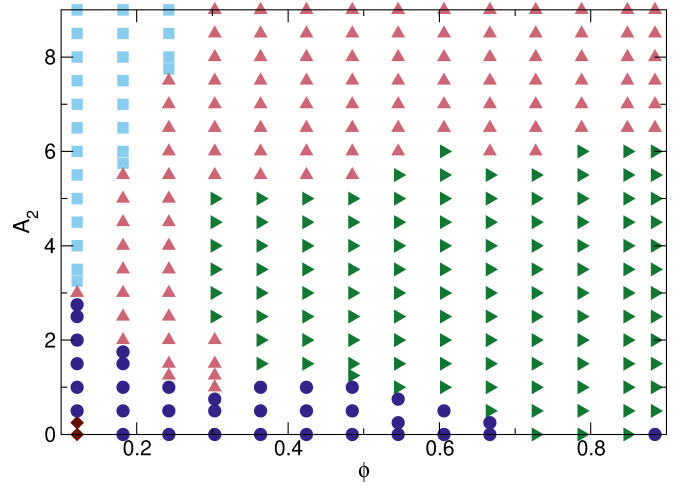


FIG. 20. Dynamic phase diagram as a function of  $A_2$  vs  $\phi$  for the system in Figs. 18 and 19 in which species one is circularly driven with  $A = 1.5$  and species two has a  $y$ -direction ac drive that is out of phase with the species one motion. Dark blue circles: initially reversible state. Light blue squares: reversible pattern forming state. Green triangles: fully phase separated state. Dark red diamonds: mixed laning state. Dark pink triangles: fluctuating liquid state. We note that the fully phase separated states at the higher values of  $A_2$  and  $\phi$  have edge transport.

amined several cases where we vary both  $A$  and  $A_2$  and find similar phases, including complete phase separation for  $\phi < 0.5$  in which stripes form that are parallel to the  $x$  direction, a configuration that is distinct from the  $y$  direction stripes that form when the drives of the two species are in phase.

## V. SUMMARY

We examine a binary assembly of two-dimensional disks at an overall disk density  $\phi$  in which one disk species undergoes chiral motion under a clockwise circular drive while the second disk species is passive. We find a rich variety of distinct pattern forming and dynamical states. As we vary the disk density and the radius of the active disk orbit, the system is generally initially in a fluctuating state where collisions between the disk species occur, and then it gradually organizes into either a reversible state or a steady fluctuating state. At low disk densities, there are no disk collisions in the reversible state, and the system forms labyrinth patterns that become coarser as the active orbit radius increases. We identify a critical orbit radius at which the time required for the system to reach a collision-free reversible state diverges as a power law with exponent  $\nu = -1.236$ , a value that is close to what is expected for a conserved directed percolation transition. This behavior is similar to that found in other periodically driven systems that organize to reversible states. For higher disk densities,



the system forms completely phase separated states that can either be reversible or exhibit edge currents or directed transport along the boundaries between the two phases. The direction of the edge current is controlled by the chirality of the active disks. We identify several reversible phases in which collisions or contact between the disks continues to occur, and show that these can be pattern forming states or a reversible jammed state. For the case in which one disk species undergoes circular driving while the second disk species is not passive but experiences a  $y$ -direction ac drive, we show that different types of phases can occur depending on whether the ac drive and circular drive are in or out of phase. These states include various types of laned structures as well as fully phase separated states and reentrant reversible phases.

This work was supported by the US Department of Energy through the Los Alamos National Laboratory. Los Alamos National Laboratory is operated by Triad National Security, LLC, for the National Nuclear Security Administration of the U. S. Department of Energy (Contract No. 892333218NCA000001).

- <sup>1</sup>C. Reichhardt and C.J.O. Reichhardt, Depinning and nonequilibrium dynamic phases of particle assemblies driven over random and ordered substrates: a review, *Rep. Prog. Phys.* **80**, 026501 (2017).
- <sup>2</sup>D.J. Pine, J.P. Gollub, J.F. Brady, and A.M. Leshansky, Chaos and threshold for irreversibility in sheared suspensions, *Nature (London)* **438**, 997 (2005).
- <sup>3</sup>C. Reichhardt and C. J. O. Reichhardt, Dynamical freezing of active matter, *Proc. Natl. Acad. Sci. (USA)* **108**, 19099 (2011).
- <sup>4</sup>V. Schaller, C.A. Weber, B. Hammerich, E. Frey, and A.R. Bausch, Frozen steady states in active systems, *Proc. Natl. Acad. Sci. (USA)* **108**, 19183 (2011).
- <sup>5</sup>C. Reichhardt and C. J. Olson Reichhardt, Absorbing phase transitions and dynamic freezing in running active matter systems, *Soft Matter* **10**, 7502 (2014).
- <sup>6</sup>K. A. Takeuchi, M. Kuroda, H. Chaté, and M. Sano, Directed percolation criticality in turbulent liquid crystals, *Phys. Rev. Lett.* **99**, 234503 (2007).
- <sup>7</sup>H. Hinrichsen, Non-equilibrium critical phenomena and phase transitions into absorbing states, *Adv. Phys.* **49**, 815 (2000).
- <sup>8</sup>L. Corte, P.M. Chaikin, J.P. Gollub, and D.J. Pine, Random organization in periodically driven systems, *Nature Phys.* **4**, 420 (2008).
- <sup>9</sup>N. Mangan, C. Reichhardt, and C. J. Olson Reichhardt, Reversible to irreversible flow transition in periodically driven vortices, *Phys. Rev. Lett.* **100**, 187002 (2008).
- <sup>10</sup>S. Okuma, Y. Tsubawa, and A. Motohashi, Transition from reversible to irreversible flow: Absorbing and depinning transitions in a sheared-vortex system, *Phys. Rev. B* **83**, 012503 (2011).
- <sup>11</sup>G. Shaw, P. Mandal, S. S. Banerjee, A. Niazi, A. K. Rastogi, A. K. Sood, S. Ramakrishnan, and A. K. Grover, Critical behavior at depinning of driven disordered vortex matter in 2H-NbS<sub>2</sub>, *Phys. Rev. B* **85**, 174517 (2012).
- <sup>12</sup>J. R. Royer and P. M. Chaikin, Precisely cyclic sand: Self-organization of periodically sheared frictional grains, *Proc. Natl. Acad. Sci. (USA)* **112**, 49 (2015).
- <sup>13</sup>C. Ness, R. Mari, and M. E. Cates, Shaken and stirred: Random organization reduces viscosity and dissipation in granular suspensions, *Sci. Adv.* **4**, eaar3296 (2018).
- <sup>14</sup>I. Regev, T. Lookman, and C. Reichhardt, Onset of irreversibility and chaos in amorphous solids under periodic shear, *Phys. Rev. E* **88**, 062401 (2013).
- <sup>15</sup>N. C. Keim and P. E. Arratia, Mechanical and microscopic properties of the reversible plastic regime in a 2D jammed material, *Phys. Rev. Lett.* **112**, 028302 (2014).
- <sup>16</sup>I. Regev, J. Weber, C. Reichhardt, K. A. Dahmen, and T. Lookman, Reversibility and criticality in amorphous solids, *Nat. Commun.* **6**, 8805 (2015).
- <sup>17</sup>P. Leishangthem, A. D. S. Parmar, and S. Sastry, The yielding transition in amorphous solids under oscillatory shear deformation, *Nat. Comms.* **8**, 14653 (2017).
- <sup>18</sup>M. O. Lavrentovich, A. J. Liu, and S. R. Nagel, Period proliferation in periodic states in cyclically sheared jammed solids, *Phys. Rev. E* **96**, 020101 (2017).
- <sup>19</sup>D. Hexner and D. Levine, Hyperuniformity of critical absorbing states, *Phys. Rev. Lett.* **114**, 110602 (2015).
- <sup>20</sup>E. Tjhung and L. Berthier, Hyperuniform density fluctuations and diverging dynamic correlations in periodically driven colloidal suspensions, *Phys. Rev. Lett.* **114**, 148301 (2015).
- <sup>21</sup>J. H. Weijs, R. Jeanneret, R. Dreyfus, and D. Bartolo, Emergent hyperuniformity in periodically driven emulsions, *Phys. Rev. Lett.* **115**, 108301 (2015).
- <sup>22</sup>J. D. Paulsen, N. C. Keim, and S. R. Nagel, Multiple transient memories in experiments on sheared non-Brownian suspensions, *Phys. Rev. Lett.* **113**, 068301 (2014).
- <sup>23</sup>N. C. Keim, J. Paulsen, Z. Zeravcic, S. Sastry, S. R. Nagel, Memory formation in matter, arXiv:1810.08587 (unpublished).
- <sup>24</sup>Y. Fily and M.C. Marchetti, Athermal phase separation of self-propelled particles with no alignment, *Phys Rev Lett* **108**, 235702 (2012).
- <sup>25</sup>G. S. Redner, M. F. Hagan, and A. Baskaran, Structure and dynamics of a phase-separating active colloidal fluid, *Phys. Rev. Lett.* **110**, 055701 (2013).
- <sup>26</sup>C. Bechinger, R. Di Leonardo, H. Löwen, C. Reichhardt, G. Volpe, and G. Volpe, Active Brownian particles in complex and crowded environments, *Rev. Mod. Phys.* **88**, 045006 (2016).
- <sup>27</sup>H. Löwen, Chirality in microswimmer motion: From circle swimmers to active turbulence, *Eur. Phys. J. Spec. Top.* **225**, 2319 (2016).
- <sup>28</sup>W.R. DiLuzio, L. Turner, M. Mayer, P. Garstecki, D.B. Weibel, H.C. Berg, and G.M. Whitesides, Escherichia coli swim on the right-hand side, *Nature (London)* **435** 1271 (2005).
- <sup>29</sup>F. Kümmel, B. ten Hagen, R. Wittowski, I. Buttinoni, R. Eichhorn, G. Volpe, H. Löwen, and C. Bechinger, Circular motion of asymmetric self-propelling particles, *Phys. Rev. Lett.* **110**, 198302 (2013).
- <sup>30</sup>M. Han, J. Yan, S. Granick, and E. Luijten, Effective temperature concept evaluated in an active colloid mixture, *Proc. Natl. Acad. Sci. (USA)* **114**, 7513 (2017).
- <sup>31</sup>H.P. Nguyen, D. Klotz, M. Engel, and S. C. Glotzer, Emergent collective phenomena in a mixture of hard shapes through active rotation, *Phys. Rev. Lett.* **112**, 075701 (2014).
- <sup>32</sup>D. Banerjee, A. Souslov, A. G. Abanov, and V. Vitelli, Odd viscosity in chiral active fluids, *Nat. Commun.* **8**, 1573 (2017).
- <sup>33</sup>A. Aubret, M. Youssef, S. Sacanna and J. Palacci, Targeted assembly and synchronization of self-spinning microgears, *Nat. Phys.* **14**, 1114 (2018).
- <sup>34</sup>B. C. van Zuiden, J. Paulose, W. T. M. Irvine, D. Bartolo, and V. Vitelli, Spatiotemporal order and emergent edge currents in active spinner materials, *Proc. Natl. Acad. Sci. (USA)* **113**, 12919 (2016).
- <sup>35</sup>G. Kokot, S. Das, R. G. Winkler, G. Gompper, I. S. Aranson, and A. Snezhko, Active turbulence in a gas of self-assembled spinners, *Proc. Natl. Acad. Sci. (USA)* **114**, 12870 (2017).
- <sup>36</sup>P. Tierno, T. Johansen, and T. Fischer, Localized and delocalized motion of colloidal particles on a magnetic bubble lattice, *Phys. Rev. Lett.* **99**, 038303 (2007).
- <sup>37</sup>C. Reichhardt and C. J. Olson Reichhardt, Dynamics and separation of circularly moving particles in asymmetrically patterned arrays, *Phys. Rev. E* **88**, 042306 (2013).
- <sup>38</sup>B. Liebchen and D. Levis, Collective behavior of chiral active matter: Pattern formation and enhanced flocking, *Phys. Rev. Lett.* **119**, 058002 (2017).

- <sup>39</sup>J. Loehr, D. de las Heras, A. Jarosz, M. Urbaniak, F. Stobiecki, A. Tomita, R. Huhnstock, I. Koch, A. Ehresmann, D. Holzinger and T. M. Fischer, Colloidal topological insulators, *Commun Phys.* **1**, 4 (2018).
- <sup>40</sup>B.-Q. Ai, Z.-G. Shao, and W.-R. Zhong, Mixing and demixing of binary mixtures of polar chiral active particles, *Soft Matter* **14**, 4388 (2018).
- <sup>41</sup>C. Scholz, M. Engel and T. Pöschel, Rotating robots move collectively and self-organize, *Nat. Commun.* **9**, 931 (2018).
- <sup>42</sup>C. Reichhardt and C. J. O. Reichhardt, Velocity force curves, laning, and jamming for oppositely driven disk systems, *Soft Matter* **14**, 490 (2018).
- <sup>43</sup>C. Reichhardt, J. Thibault, S. Papanikolaou, and C. J. O. Reichhardt, Laning and clustering transitions in driven binary active matter systems, *Phys. Rev. E* **98**, 022603 (2018).
- <sup>44</sup>E. Tjhung and L. Berthier, Criticality and correlated dynamics at the irreversibility transition in periodically driven colloidal suspensions, *J. Stat. Mech.* **2016**, 033501 (2016).
- <sup>45</sup>B. L. Brown, C. Reichhardt, and C. J. O. Reichhardt, Reversible to irreversible transitions in periodically driven skyrmion systems, arXiv:1810.06629 (unpublished).
- <sup>46</sup>K. Dasbiswas, K. K. Mandadapu, and S. Vaikuntanathan, Topological localization in out-of-equilibrium dissipative systems, *Proc. Natl. Acad. Sci. (USA)* **115**, E9031 (2018).
- <sup>47</sup>S. R. McCandlish, A. Baskaran, and M. F. Hagan, Spontaneous segregation of self-propelled particles with different motilities, *Soft Matter* **8**, 2527 (2012).
- <sup>48</sup>J. Stenhammar, R. Wittkowski, D. Marenduzzo, and M. E. Cates, Activity-induced phase separation and self-assembly in mixtures of active and passive particles, *Phys Rev Lett* **114**, 018301 (2015).
- <sup>49</sup>M. E. Cates and J. Tailleur, Motility-induced phase separation, *Ann. Rev. Condens. Matter Phys.* **6**, 219 (2015).
- <sup>50</sup>F. Alaimo and A. Voigt, Microscopic field-theoretical approach for mixtures of active and passive particles, *Phys. Rev. E* **98**, 032605 (2018).